European Review for Medical and Pharmacological Sciences 2021; 25: 1600-1611

BMSCs attenuate hepatic fibrosis in autoimmune hepatitis through regulation of LMO7-AP1-TGFβ signaling pathway

Z.-K. CHEN[1], D.-Z. CHEN[2], C. CAI[1], L.-L. JIN[1], J. XU[1], Y.-L. TU[1], X.-Z. HUANG[1], J.-L. XU[1], M.-Z. CHEN[1], F.-B. XUE[1], X.-L. LAN[3], X.-D. WANG[1], Y.-L. GE[3], H.-L SUN[3], Y.-P. CHEN[1]

[1]Department of Infectious Diseases, the First Affiliated Hospital of Wenzhou Medical University, Zhejiang Provincial Key Laboratory for Accurate Diagnosis and Treatment of Chronic Liver Diseases, Wenzhou Key Laboratory of Hepatology, Hepatology Institute of Wenzhou Medical University, Wenzhou, Zhejiang, China
[2]Department of Gastroenterology, The First Hospital of Peking University, Beijing, China
[3]Department of Infectious Diseases, Lishui People's Hospital, Lishui, China

Zhengkang Chen and Dazhi Chen contributed equally to the manuscript

Abstract. – OBJECTIVE: In a previous study, we reported that transplantation of bone mesenchymal stem cells (BMSCs) significantly attenuated liver damage in a mouse autoimmune hepatitis (AIH) model. Moreover, expression of the LIM domain protein, LMO7, correlated positively with the invasive capacity of hepatoma cells. However, whether LMO7 plays a role in inflammation and fibrosis of AIH remains unknown. This investigation aimed to explore the effect of BMSC transplantation on LMO7 and the role of LMO7 in hepatic fibrosis.

MATERIALS AND METHODS: S100-induced murine AIH and LPS-induced hepatocyte injury models were successfully established. Three doses of BMSCs were injected into AIH mice via the tail vein. LPS-treated AML12 cells were co-cultured with BMSCs *in vitro*. Small interfering (si) LMO7 RNA and T5224 (a specific inhibitor of AP-1) were used to demonstrate the relationship between LMO7-AP1-transforming growth factor (TGF)-β.

RESULTS: Pathological examination and serum alanine and aspartate aminotransferase levels indicated that liver damage was notably ameliorated in the BMSC-treated mice. LMO7 level was upregulated, while AP-1 and TGF-β levels were downregulated upon intervention with BMSCs. AP-1 expression was upregulated in the siLMO7 group, whereas TGF-β level was downregulated in the T5224 group when compared to those in the control group.

CONCLUSIONS: BMSC transplantation significantly limits liver fibrosis and upregulates the expression of LMO7. LMO7 inhibits the TGF-β pathway by inhibiting AP-1. This implies that BMSCs are a potential means of treating liver fibrosis. This approach has important implications for the treatment of AIH and other fibrotic diseases.

Key Words:
Bone mesenchymal stem cells, Hepatic fibrosis, Liver damage, Autoimmune hepatitis, LMO7.

Introduction

Autoimmune hepatitis (AIH) is a chronic and progressive liver disease that leads to cirrhosis or hepatocellular carcinoma with an etiology that remains unclear. AIH is a global disease that may affect all ethnicities and ages but is predominant in females[1]. AIH responds favorably to immunosuppressive treatments such as corticosteroids and azathioprine. However, when patients with AIH develop liver fibrosis, the anti-fibrotic response of these treatments is quite limited. Furthermore, 0.1-8.1% of AIH patients per year develop liver cirrhosis[2,3]. Therefore, there is an urgent need to develop better treatment methods to prevent liver fibrosis from developing into cirrhosis.

Bone mesenchymal stem cell (BMSC)-based therapy is a promising and increasingly common

Corresponding Authors: Yongping Chen, MD; e-mail: did@wzhospital.cn
Huiling Sun, MD; e-mail: LS2680201@163.com
Yuli Ge, MD; e-mail: gyulifly@163.com

strategy used to treat various diseases, especially liver diseases. It works through tissue repair and immune regulation[4-6]. We documented that BMSC transplantation significantly reduced inflammation and fibrosis in S100-induced AIH mice[7]. However, the potential mechanisms of tissue repair and immune regulation remained unclear.

Transforming growth factor (TGF)-β is a key cytokine that regulates extracellular matrix (ECM) deposition in many fibrotic diseases and is highly expressed in AIH[8,9]. TGF-β functions by binding to specific cell membrane receptors and then activating Smad2/3 signaling proteins. Smad2/3 proteins are imported into the nucleus, where they bind to specific DNA sequences of genes that they regulate[10]. Autoinduction of TGF-β is mediated by the transcription factor, AP-1[11]. The protein, LIM (Lin11, Isl-1, and Mec-3) domain only 7 (LMO7) has been identified as a novel negative feedback regulator of TGF-β signaling and ECM deposition. LMO7 is a 150-kDa scaffolding protein that contains several protein-protein interaction domains such as calponin homology, PDZ (PSD95, Dlg1, and ZO-1), F-Box, and LIM domains[12,13]. LMO7 localizes to different organelles in cells such as the plasma membrane, cytoskeleton, and nucleus[12]. LMO7 also mediates assembly of adherens junctions[12], cell migration[14], and gene transcription[15]. Although LMO7 appears to play a role in hepatoma cells and vascular fibrosis, its role in liver fibrosis, and its regulation by AP1 and TGF-β, remain unknown, especially in liver fibrosis of AIH.

Materials and Methods

Establishment of the Murine AIH Model

Thirty-two male wild-type C57BL/6 mice (4 to 6 weeks of age) were purchased from the Shanghai Laboratory Animal Center (Shanghai, China). The Ethics Committee approval was approved by the Wenzhou Medical University Animal Policy and Welfare Committee Ethics (Approval Document No. wydw2020-0400). For hepatic S100 preparation, after administering sodium pentobarbital anesthesia, eight mice were sacrificed. Their livers were collected after cardiac perfusion with phosphate-buffered saline (PBS), minced and homogenized, then centrifuged at 150 g for 10 min. After subsequent centrifugation at 100,000 g for 2 h, the supernatants were referred to as S100. These were concentrated to 0.5 mL using an Amicon Ultra-15 filter (EMD Millipore, Billerica, MA, USA) and subsequently passed through a 90 cm CL-6B Sepharose column (Solarbio, Revetal, Norway) with AKTA pure (GE Healthcare, Pittsburgh, PA, USA). Of the three resulting protein peaks, peaks 1 and 3 were safer components compared to peak 2. In this experiment, peak 3, at a protein concentration of 0.5 to 2 g/L, was emulsified in an equal volume of complete or incomplete Freund's adjuvant (Solarbio) on days 0 and 7, respectively. Mice were injected intraperitoneally twice on days 0 and 7 (Figure 1A).

Treatment with BMSCs In Vivo

Mouse BMSCs (P6) were purchased from Cyagen Biosciences (Guangzhou, China). Cells were grown in C57BL/6 Mouse MSC Basal Medium (Cyagen Biosciences, Guangzhou, China) containing 10% fetal bovine serum (FBS) and 1% penicillin-streptomycin and incubated at 37°C with 5% CO_2.

Twenty-four mice were divided randomly into three groups: control (n = 8), AIH model (n = 8), and AIH model + BMSC-treated (n = 8) groups. Mice in the control group were injected with only phosphate-buffered saline on days 0 and 7. Both the AIH model and BMSC treatment groups were injected with S100 on days 0 and 7. After the second injection of S100, the BMSC-treated group was injected with BMSCs via the tail vein (> 1×10^5 cells/mouse) three times: on days 21, 28, and 35. All mice were sacrificed on day 42.

Cell Culture and Co-Culture Systems

AML12 cells were maintained in Dulbecco's Modified Eagles/F12 medium (DMEM; Gibco, Gaithersburg, MD, USA) supplemented with 10% fetal bovine serum, 40 ng/mL dexamethasone at 37°C in 5% CO_2. To establish the co-culture system, 3×10^4 AML12 cells were added to a 24-well plate (Figure 1B). When the cells adhered to the bottom of the well, lipopolysaccharide (LPS) was added with the amount of 250 ng/mL, and the cells were incubated for 24 h at 37°C. BMSCs (3×10^4 cells) were added to a transwell chamber and allowed to adhere to the chamber for 4 to 6 h of incubation. The transwell chamber was then placed on a 24-well plate and co-cultured for 24 h before subsequent experiments.

Small Interfering (si)RNA Knockdown of LMO7

Non-specific control siRNA (UUCUCCGAACGUHUCACGUTT) and siRNA for LMO7 (CCAACTGACAGGAGTAAAT) were purchased from RiboBio (Guangzhou, China). AML12 cells

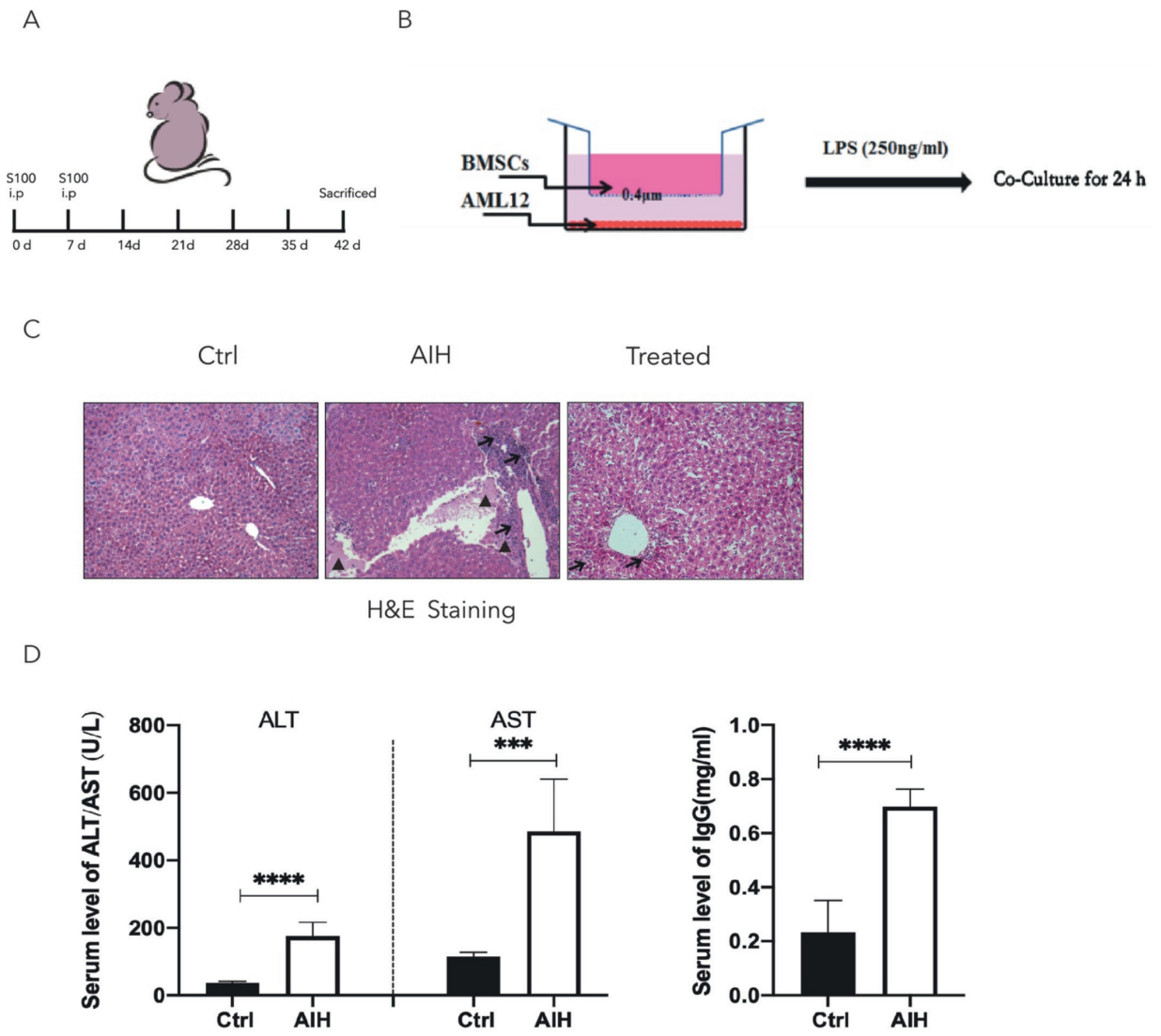

Figure 1. Establishment of the mouse autoimmune hepatitis (AIH) model. **A,** Treatment schedule to establish the AIH model. **B,** Flow chart of the co-culture system. **C,** Hematoxylin and eosin (H&E) staining of liver tissues showing structural differences between the control, AIH, and bone mesenchymal stem cell (BMSC) treated groups. The black arrows highlight lymphocytic infiltration. The black triangles highlight hepatocyte necrosis (magnification: ×200). **D,** Serum levels of alanine aminotransferase (ALT) and aspartate aminotransferase (AST) in the control and AIH groups. IgG levels in mouse serum in control and AIH groups were determined by an enzyme-linked immunosorbent assay. Ctrl, control. Data are presented as means ± SE from six or eight mice. ***$p < 0.001$, ****$p < 0.0001$.

were transfected with non-specific control siRNA or LMO7-specific knockdown siRNA using Lipofectamine™ 2000 (Thermo Fisher Scientific, Waltham, MA, USA) according to the manufacturer's protocol. The following four groups were established: control, LPS, siLMO7, and siLMO7 + LPS.

Inhibition of AP-1

T-5224 is a novel, non-peptide, small molecule inhibitor of c-Fos/AP-1. When AML12 cells reached 80-90% confluence, T-5224 was added. After 12 h, the cells were incubated with 250 ng/mL LPS for another 24 h.

Liver Histopathology

After harvesting, liver tissue of mice was fixed with 4% paraformaldehyde, then embedded in paraffin and sliced into 5-μm thick sections. Tissue sections were stained with hematoxylin-eosin, Sirius Red, and Masson's trichrome dyes, and the inflammation, fibrosis, and structural changes were observed under a Nikon light microscope.

Serum Measurements

Blood samples were centrifuged at 1500 rpm for 10 min to obtain the serum, which was flash frozen for further analyses. Serum aspartate aminotransferase (AST) and alanine aminotransferase (ALT) levels were measured using an automated biochemical analyzer (Abbott Laboratories, Lake Forest, IL, USA). The IgG content was determined using a mouse enzyme-linked immunoassay kit (LiankeBio, Hangzhou, China) according to the manufacturer's protocol.

Western Blotting

The total protein extract of liver tissue or cells was separated with supplementary lytic buffer and quantified using a bicinchoninic acid (BCA) protein analysis kit (Beyotime, Haimen, China). The protein sample (20 μg) was denatured by heating at 100°C for 10 min. Protein lysates were separated on a 10% sodium dodecyl sulfate-polyacrylamide gel (SDS-PAGE) and transferred to polyvinylidene difluoride (PVDF) membranes. The membranes were first blocked with 5% bovine serum albumin (BSA) in tris-buffered saline/0.1% Tween 20 (TBST-20) for 2 h, then incubated with the following specific antibodies: LMO7 (ab200675), AP-1 (ab21981), lamin B (ab133741), GADPH (ab8245), collagen-1 (COL-1) (ab3476), TGF-β (ab27969), and α-smooth muscle actin (α-SMA) (ab32575) from Abcam (Cambridge, UK) at 4°C for 12 h. The membranes were washed and then incubated with a goat anti-rabbit secondary antibody (1:5000, Biosharp, Anhui, China) at room temperature for 1 h. The membranes were captured as digital images on a ChemiDoc immunoblot detection system (Bio-Rad, Hercules, CA, USA). ImageJ software (National Institutes of Health, Bethesda, MD, USA) was used to quantify the bands.

Quantitative Real-Time Polymerase Chain Reaction (qRT-PCR)

Total RNA was isolated from frozen liver tissue or cultured cells using TRIzol reagent, and the cDNA was reverse-transcribed using the PrimeScript™ RT-PCR reagent kit (TaKaRa Bio, Otsu, Shiga, Japan, DRR037A). QRT-PCR was performed using TB Green Premix Ex Taq™ II (Takara Bio, RR820A) in an ABI7500 Fast Real-Time PCR system (Applied Biosystems, Foster City, CA, USA). The primer sequences are listed in Table I. mRNA expression was normalized to the expression of GAPDH using the $2^{-\Delta\Delta}$CT method.

Statistical Analysis

Statistical analyses were performed using Prism 8.0 software (GraphPad, La Jolla, CA, USA). Data are expressed as means ± SE. For multiple group comparisons, a one-way analysis of variance with Tukey's or Dunnett's post-hoc test was used. p-values of < 0.05 were considered statistically significant.

Results

Establishment of the Murine AIH Model

In Figure 1A, we display the flow chart of the procedure used to induce AIH in mice. Mice were injected intraperitoneally with S100 on days 0 and 7. Compared to the control group, hematoxylin and eosin staining showed pathological changes, including massive infiltration of lymphocytes and hepatocyte necrosis, in the liver tissue of S100-treated mice (Figure 1C). In addition, serum ALT/AST and IgG levels were elevated in the model group (Figure 1D). This implies that the AIH model was successfully established.

BMSCs Diminish Liver Inflammation and Fibrosis In Vivo and In Vitro

BMSCs were transplanted on days 21, 28, and 35 after S100 injection via tail vein injection. All animals were sacrificed on day 42 (Figure 2A). After BMSC transplantation, the levels of inflammatory cytokines and intracellular signaling molecules were examined. There was a significant increase in interleukin (IL)-6 and IL-11 mRNA levels in liver tissue of the AIH group, and BMSC treatment ameliorated these levels (Figure 2B). Serum ALT/AST levels in BMSC-treated mice were lower when compared to those in the AIH group (Figure 2C).

BMSC treatment not only reduced destruction of the lobular structure with no visible hepatocyte necrosis and lymphocyte infiltration (Figure 1C), but also attenuated the development of liver fibrosis as shown by Masson's trichrome and Sirius Red staining (Figure 3A). Moreover, fibrosis parameters, such as the protein and mRNA levels of COL-1, α-SMA, and TGF-β, were increased in the liver tissues of AIH mice compared to control mice and mice treated with BMSCs (Figure 3B, C). Furthermore, the protein levels of LMO7 and AP-1 were decreased and increased, respectively, in the AIH group, but BMSC transplantation elevated the levels of LMO7 and reduced those of AP-1 (Figure 3B).

Table I. The primer sequences of genes in real-time qPCR assays.

TGF-β1 forward	CAACCCAGGTCCTTCCTAAA
TGF-β1 reverse	GGAGAGCCCTGGATACCAAC
COL-1 forward	TGCCGTGACCTCAAGATGTG
COL-1 reverse	CACAAGCGTGCTGTAGGTGA
α -SMA forward	GTGCTATGTCGCTCTGGACTTTGA
α -SMA reverse	ATGAAAGATGGCTGGAAGAGGGTC
IL-6 forward	GGCAAGCCTTCCAGTTAGTCTTCC
IL-6 reverse	AGAGTAAGCGTCCAGAGGTCAGC
IL-11 forward	CAGGAGTATGCCGAAAGG
IL-11 reverse	CCCCAGAAAGCCTAGATTG
GAPDH forward	CTCTCCCTCACGCCATC
GAPDH reverse	ACGCACGATTTCCCTCTC

The expression of all these proteins was also examined in a cell culture system. AML12 cells were co-cultured with BMSCs (Figure 1B). As shown in Figure 4A, mRNA levels of IL-6 and IL-11 were increased in LPS-treated cells, while BMSCs reversed this LPS-induced elevation. Moreover, the levels of COL-1, α-SMA, and TGF-β were significantly increased after LPS treatment, while BMSC co-culture reversed the LPS-induced elevation of these markers (Figure 4B, C). LMO7 and AP-1 were also examined in the co-culture system. LMO7 expression was reduced, and AP-1 was elevated after LPS treatment. However, BMSC co-culture increased LMO7 levels, while it reduced the AP-1 levels (Figure 4B). These findings are consistent with observations in liver tissue of AIH mice.

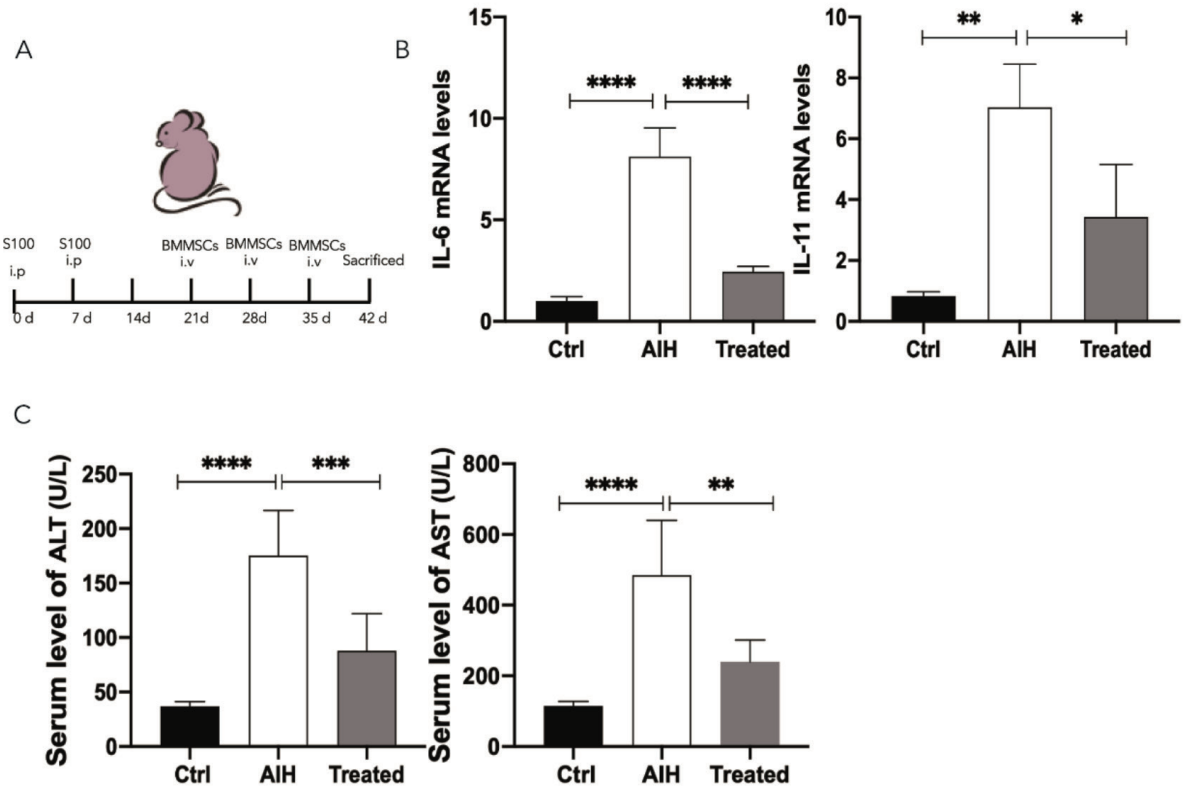

Figure 2. Bone mesenchymal stem cells (BMSCs) mediate inflammation and liver function in autoimmune hepatitis (AIH) model mice. **A,** Time-points of BMSC injection. **B,** Interleukin (IL)-6 and IL-11 mRNA levels in liver tissues of each group. **C,** Serum levels of alanine aminotransferase (ALT) and aspartate aminotransferase (AST) in each group. Ctrl, control. Data are presented as means ± SE from six or eight mice. *$p < 0.05$, **$p < 0.01$, ***$p < 0.001$, ****$p < 0.0001$.

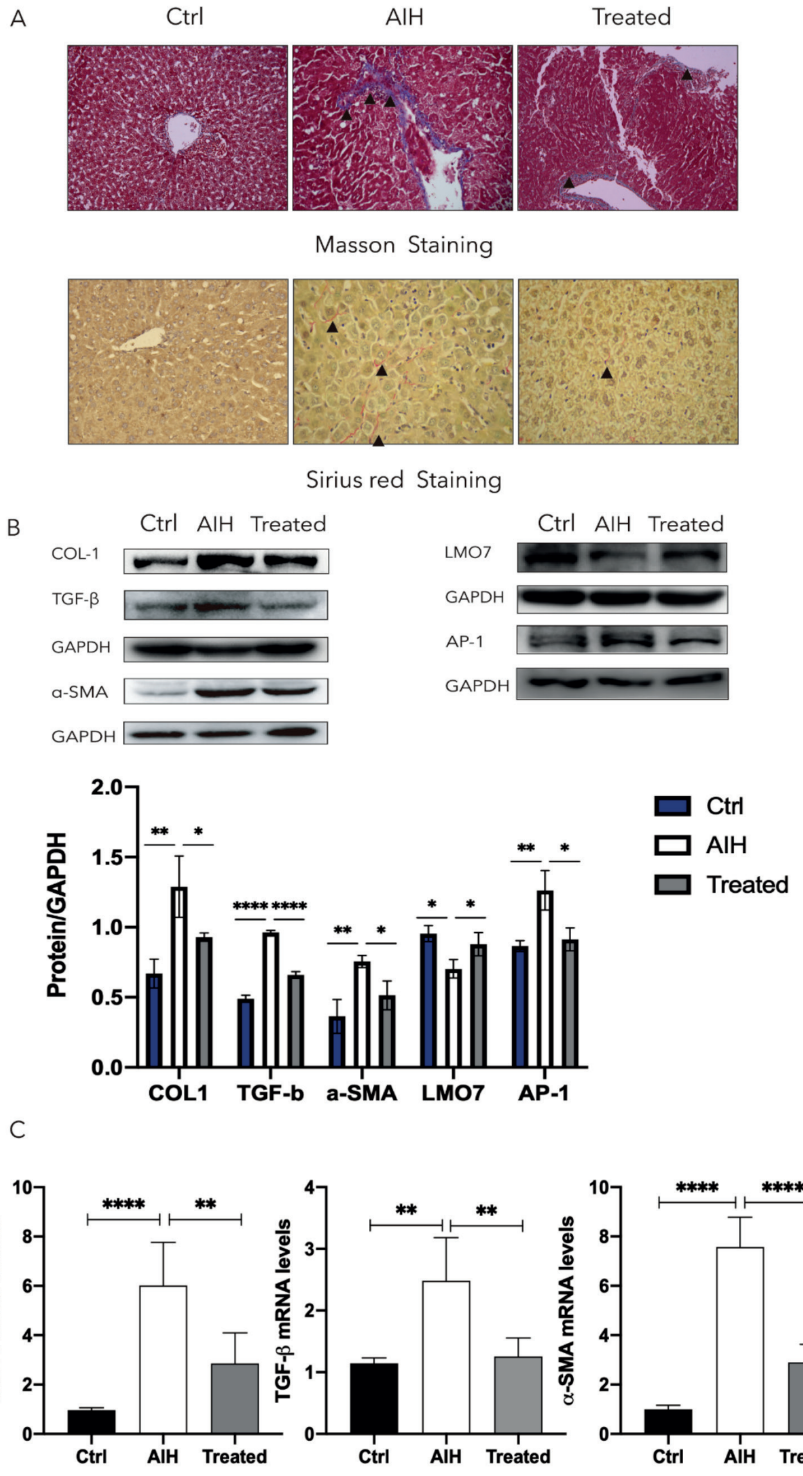

Figure 3. Bone mesenchymal stem cells (BMSCs) attenuate liver fibrosis in autoimmune hepatitis (AIH) model mice. **A,** Micrographs of Masson's trichrome and Sirius Red staining in each group. Black triangles highlight hepatocyte necrosis (magnification: Masson's trichrome ×200; Sirius Red ×400). **B,** Western blot analyses of collagen-1 (COL-1), α-smooth muscle actin (α-SMA), transforming growth factor (TGF)-β, LMO7, and AP-1 in liver tissues. GAPDH was used as the loading control. The lower panel shows the densitometric quantification for panel B. **C,** COL-1, α-SMA, and TGF-β mRNA levels in liver tissues, normalized to the levels of GAPDH. Ctrl, control. Data are presented as means ± SE from six or eight mice. *$p < 0.05$, **$p < 0.01$, ***$p < 0.001$, ****$p < 0.0001$.

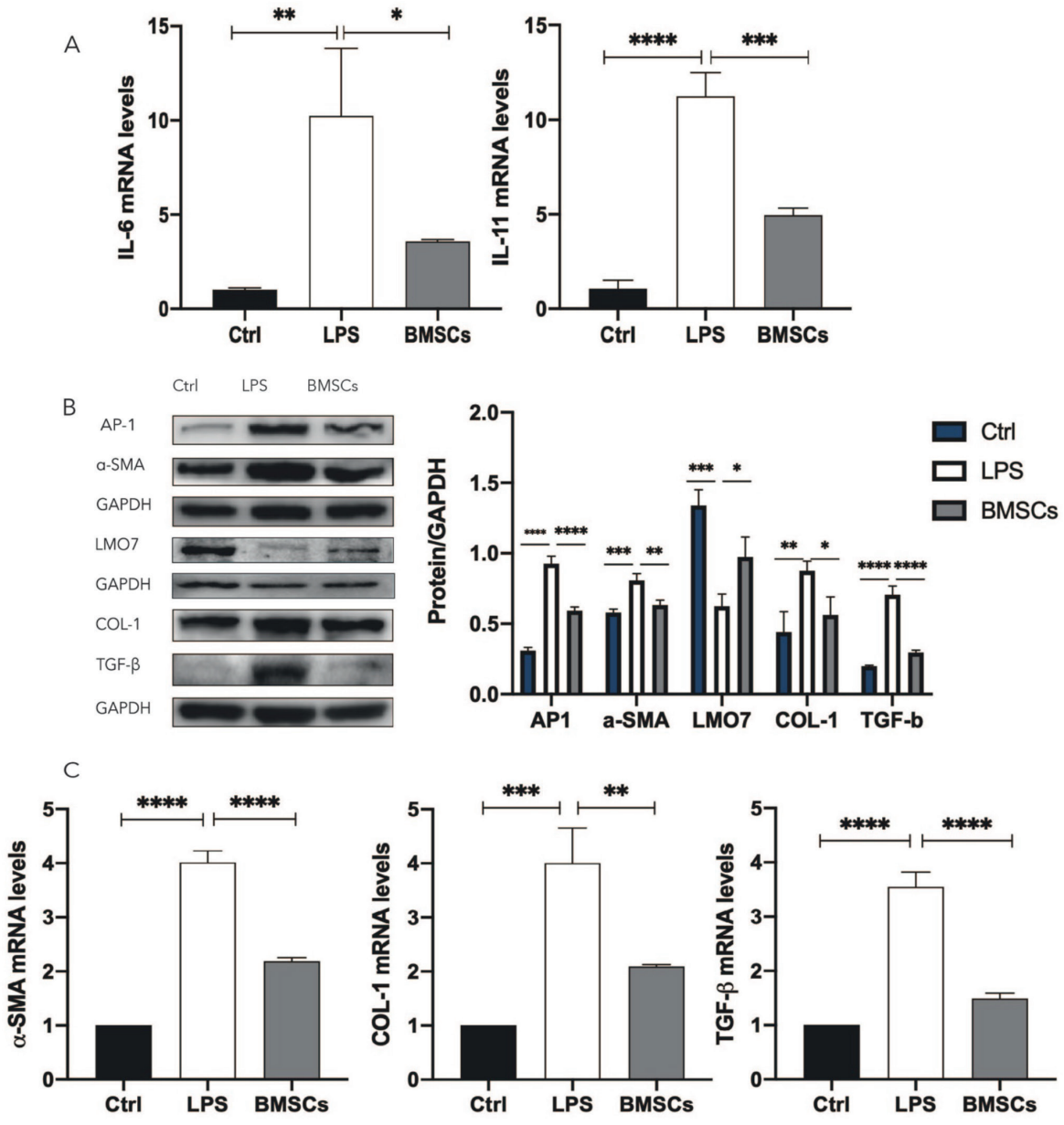

Figure 4. Bone mesenchymal stem cells (BMSCs) attenuate lipopolysaccharide (LPS)-induced injury in AML12 cells. **A,** Interleukin (IL)-6 and IL-11 mRNA levels in AML12 cells, normalized to the levels of GAPDH. **B,** Western blot analyses of collagen-1 (COL-1), α-smooth muscle actin (α-SMA), transforming growth factor (TGF)-β, LMO7, and AP-1 on AML12 cells, normalized to the levels of GADPH. The right panel shows the densitometric quantification for panel B. **C,** COL-1, α-SMA, and TGF-β mRNA levels in AML12 cells, normalized to the levels of GAPDH. Ctrl, control. Data are presented as means ± SE from three independent experiments. *$p < 0.05$, **$p < 0.01$, ***$p < 0.001$, ****$p < 0.0001$.

LMO7 is a Protective Factor in LPS-Treated AML12 Cells

To demonstrate the function of LMO7, siRNA targeting LMO7 was used to inhibit its expression (Figure 5A). The protein and mRNA levels of COL-1, α-SMA, and TGF-β increased after incubation of AML12 cells with 250 ng/mL of LPS for 24 h (Figure 5B, C). The addition of LMO7 siRNA after LPS treatment further increased these levels. Furthermore, LPS elevated AP-1, and the addition of LMO7 siRNA also increased this level further (Figure 5B).

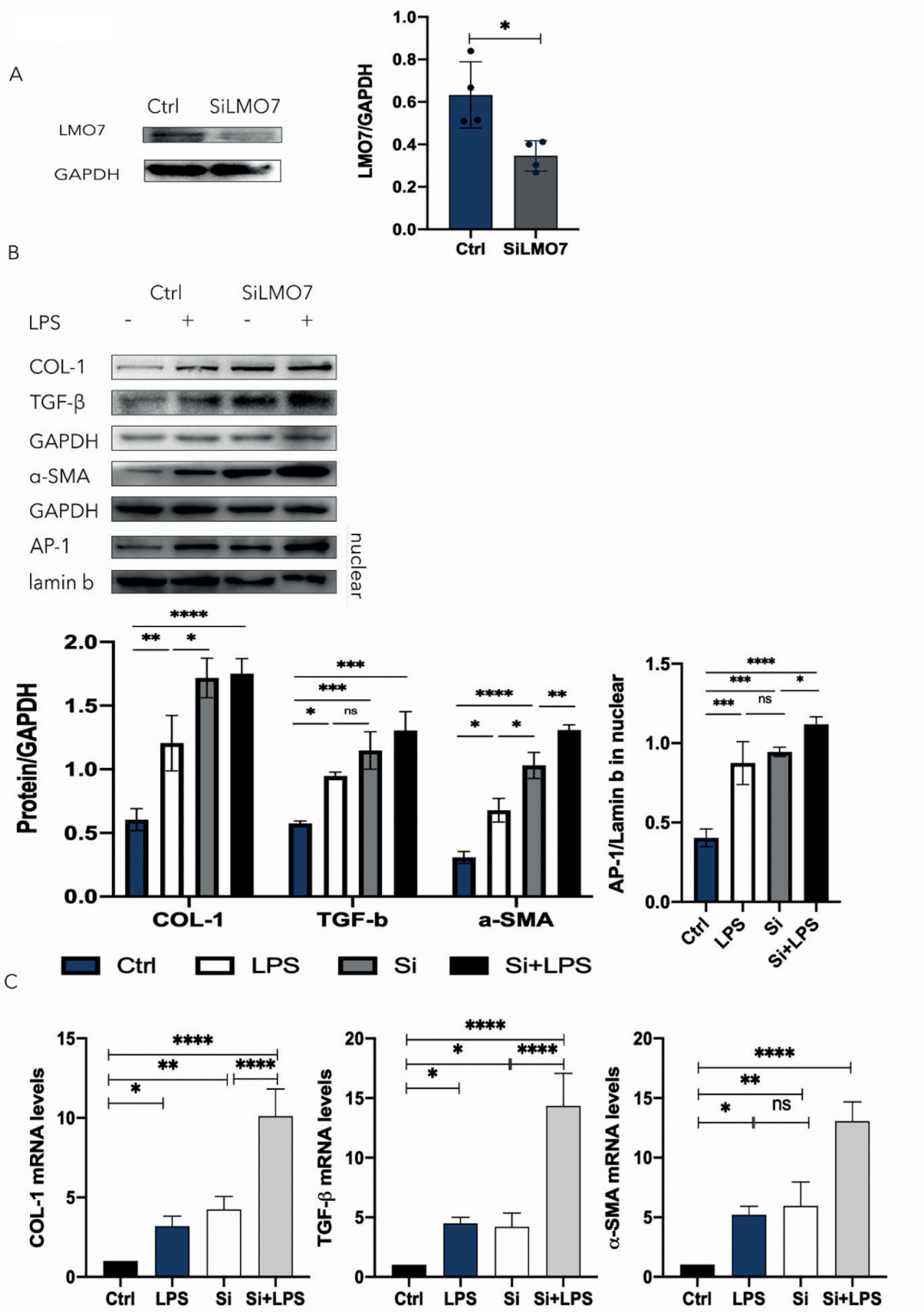

Figure 5. LMO7 inhibits AP-1 activity in lipopolysaccharide (LPS)-treated AML12 cells. **A,** Western blot analysis of LMO7 in AML12 cells. GAPDH was used as the loading control. The LMO7 protein level is decreased by small interfering (si)RNA. The right panel shows the densitometric quantification for panel A. **B,** Western blot analyses of collagen-1 (COL-1), α-smooth muscle actin (α-SMA), transforming growth factor (TGF)-β, and AP-1 (nuclear) protein levels in AML12 cells. GAPDH and lamin B were used as loading controls. The lower panels show the densitometric quantification for panel B. **C,** COL-1, α-SMA, and TGF-β mRNA levels in AML12 cells, normalized to the levels of GAPDH. Ctrl, control. Data are presented as means ± SE from three independent experiments. *$p < 0.05$, **$p < 0.01$, ***$p < 0.001$, ****$p < 0.0001$.

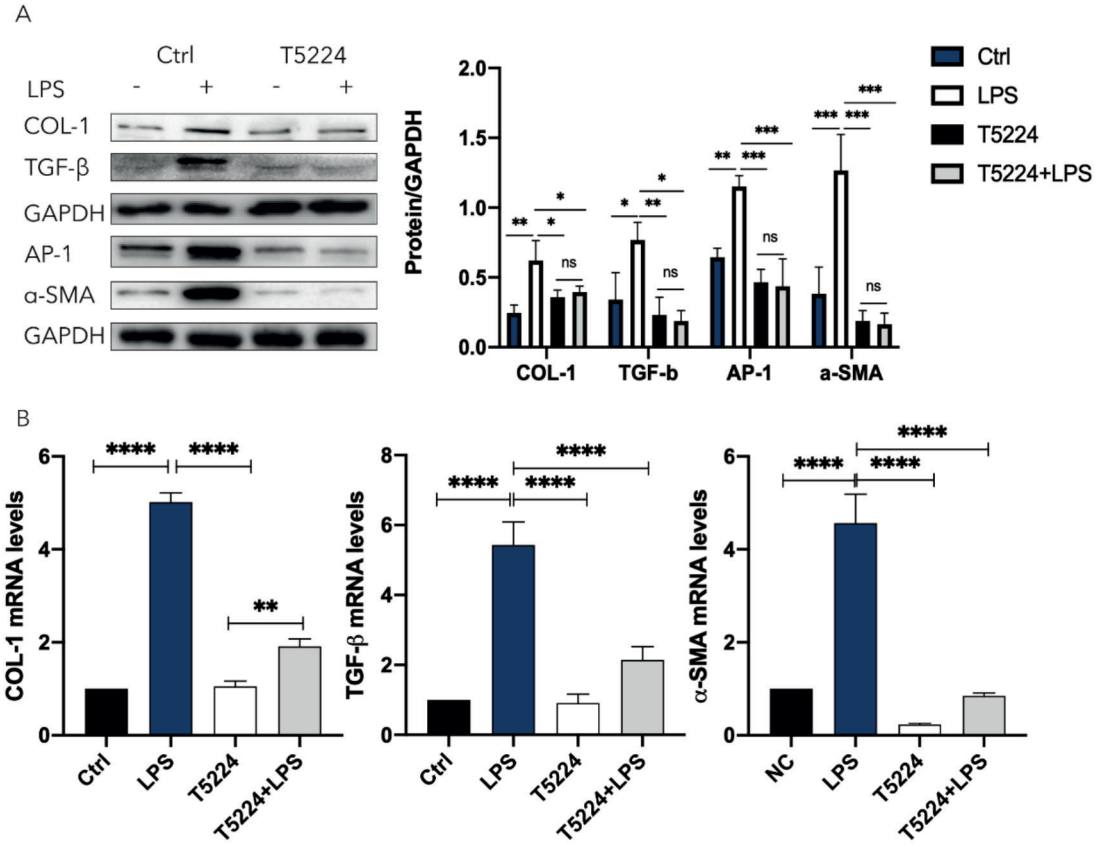

Figure 6. AP-1 exacerbates lipopolysaccharide (LPS)-induced fibrosis. **A,** AP-1 is inhibited by T5224. Immunoblot analysis of collagen-1 (COL-1), α-smooth muscle actin (α-SMA), transforming growth factor (TGF)-β, and AP-1 protein levels in AML12 cells. GAPDH was used as the loading control. The right panel shows the densitometric quantification for panel A. **B,** COL-1, α-SMA, and TGF- β mRNA levels in AML12 cells, normalized to the levels of GAPDH. Ctrl, control. Data are presented as means ± SE from three independent experiments. *$p < 0.05$, **$p < 0.01$, ***$p < 0.001$, ****$p < 0.0001$.

Effect of Inhibiting AP-1 in AML12 Cells

AP-1 is a transcription factor thought to be associated with inflammation and carcinomas. To determine whether AP-1 played a role in LPS-treated AML12 cells, T5224, an inhibitor of AP-1, was incubated with AML12 cells with and without LPS treatment for 24 h. As shown in Figure 6A and B, the protein and mRNA levels of COL-1, α-SMA, and TGF-β were significantly increased in cells treated with LPS alone, whereas these increases were prevented by T5224.

Discussion

AIH is a chronic liver disease caused by immune disorders and may lead to liver damage and cirrhosis. Immunosuppressive treatments remain the mainstream therapy. Prednisone, with or without azathioprine, is a standard therapy that is effective for most patients: 38-93% of patients show improvement[16,17]. Continued immunosuppressive treatment can reduce the risk of AIH recurrence for at least 5 years. However, immunosuppressive treatments have limitations. According to relevant studies, long-term corticosteroid therapy is associated with weight gain and vascular disease, while also increasing the risk of diabetes and low-trauma fractures[18]. Moreover, the progression of fibrosis cannot be completely stopped with this therapy; 30-50% of patients still develop cirrhosis[19]. Unfortunately, over the last few decades, there are only a few major advances reported in the treatment of AIH.

BMSC transplantation is effective in decreasing liver fibrosis in mice and is a promising treat-

ment in clinical trials for many liver diseases[20,21]. In our previous research, BMSCs were effective in ameliorating liver inflammation and fibrosis in S100-induced AIH[7], but the potential mechanism was poorly understood. The TAK1 pathway plays an essential role in hepatic inflammation and fibrosis in the S100-induced AIH model[22]. AP-1 is a transcription factor downstream of TAK1 that contributes to smooth muscle cell proliferation[23] and increases TGF-β1 and integrin β3 gene transcription[24]. Furthermore, LMO7 inhibits AP-1 activity and TGF-β1 autoinduction, and in a vascular injury model, neointimal formation, ECM deposition, and proliferation were enhanced in LMO7 knockout compared with wild-type mice[25].

In the current study, we confirmed that BMSC transplantation influenced S100-induced liver inflammation and fibrosis in a murine model, as well as LPS-treated AML12 cells in a co-culture system. The *in vivo* and *in vitro* results were consistent, which implies that BMSCs may play a therapeutic role by secreting beneficial substances. For example, MSC-exosomes have been used as carriers to deliver microRNAs into cells and promote hepatic regeneration in a model of autoimmune hepatitis[26], and Tan et al[27] demonstrated that, in a drug-induced liver injury model, treatment with MSC-exosomes can be helpful in hepatic repair.

In the current investigation, over-expression of AP-1 was found in the AIH group, and this was prevented in the BMSC-treated group. Furthermore, after treatment with a specific inhibitor of AP-1, inflammation and fibrosis were significantly reduced, so AP-1 may be used as a helpful biomarker and therapeutic target. AP-1 is an intracellular transcriptional activator that is mainly composed of c-Jun and c-Fos proteins encoded by proto-oncogenes. AP-1 is closely related to immune diseases and carcinomas and is considered to be an important regulator. Over-expression of AP-1 is found in rheumatoid arthritis and long-term allogeneic hematopoietic stem cell transplantation survivors[28]. Since AIH is highly related to immune disorders, and BMSCs have a strong ability to suppress inflammation and autoimmunity[29], one of the limitations of the present study is that immune disorders and changes after BMSC transplantation were not documented; therefore, the underlying mechanism may be worthy of exploration.

Several reports[30,31] suggest that the expression of LMO7 is markedly upregulated in various human cancers and is able to enhance the invasiveness of rat ascites hepatoma cells. LMO7 is induced by TGF-β, which restricts the TGF-β pathway through negative feedback regulation, thus limiting vascular fibrosis[25]. We found that LMO7 was decreased in the AIH group and increased in the BMSC-treated group. This suggests a protective role for LMO7 in liver fibrosis. When LMO7 levels were downregulated by siRNA, AP-1 was upregulated in the nucleus, suggesting a connection between AP-1 and LMO7. Indeed, LMO7 interferes with AP-1-dependent transcriptional self-induction of TGF-β. The LIM domain of LMO7, known for its scaffolding activity, interacts with c-Fos and c-Jun and promotes their ubiquitination and degradation. In addition, Xie et al[25] mutated the C-terminal LIM domain region of LMO7 and found that full-length LMO7, but not the C-terminal mutant, co-immunoprecipitated with c-Fos or c-Jun in HEK293A cells. Functionally, full-length LMO7, but not the C-terminal mutant, inhibited the expression of Jun, Fos, TGF-β1, integrin, and ECM mRNAs. This suggests that the C-terminal LIM domain region of LMO7 is required for interaction with, and degradation of, c-FOS and c-JUN.

Conclusions

Our results show that BMSCs attenuate inflammation and fibrosis both *in vivo* and *in vitro*. Moreover, about the novelty of this investigation, this article verified that the LMO7 and AP-1 pathways may mediate the regulation of inflammation and fibrosis by BMSCs; LMO7 inhibits the TGF-β pathway by inhibiting AP-1. This implies that BMSCs are a potential means of treating liver fibrosis. Furthermore, the precise roles and functions of LMO7 are still unclear; however, LMO7 and AP-1 can be a potential therapeutic target.

Acknowledgments

The authors would like to thank Ruicong Chen for excellent technical support and for critically reviewing the manuscript.

Conflict of Interest

We declare that we have no financial and personal relationships with other people or organizations that can inappropriately influence our work; there is no professional or other personal interest of any nature or kind in any product, service, or company that could be construed as influencing the position presented in, or the review of, the present manuscript.

Statement of Interests

This work received financial support from the National Natural Science Foundation of China (NSFC) (Grant No. 81570514, 81770585, and 81600466), the National Science and Technology Major Project (Grant No. 2017ZX10202201, 2017ZX10203201, and 2018ZX10725506-001), Project of Zhejiang Provincial Department of Health, China (2018KY929), and Zhejiang Provincial Natural Science Foundation of China (LGF19H030010).

References

1) Mieli-Vergani G, Vergani D, Czaja AJ, Manns MP, Krawitt EL, Vierling JM, Lohse AW, Montano-Loza AJ. Autoimmune hepatitis. Nat Rev 2018; 4: 18017.
2) Poulsen LO, Thulstrup AM, Mellemkjaer L, Vilstrup H, Sørensen HT. Mortality and causes of death in patients with "lupoid hepatitis." A long-term follow-up study in Denmark. Can Med Bull 2002; 49: 263-265
3) Hino T, Kumashiro R, Ide T, Koga Y, Ishii K, Tanaka E, Morita Y, Hisamochi A, Murashima S, Tanaka K, Ogata K, Kuwahara R, Sata M; Autoimmune Hepatitis Study Group. Predictive factors for remission and death in 73 patients with autoimmune hepatitis in Japan. Int J Mol Med 2003; 11: 749-755.
4) Kim MD, Kim SS, Cha HY, Jang SH, Chang DY, Kim W, Suh-Kim H, Lee JH. Therapeutic effect of hepatocyte growth factor-secreting mesenchymal stem cells in a rat model of liver fibrosis. Exp Mol Med 2014; 46: e110.
5) Christ B, Brückner S, Winkler S. The therapeutic promise of mesenchymal stem cells for liver restoration. Trends Mol Med 2015; 21: 673-686.
6) Volarevic V, Nurkovic J, Arsenijevic N, Stojkovic M. Concise review: therapeutic potential of mesenchymal stem cells for the treatment of acute liver failure and cirrhosis. Stem Cells 2014; 32: 2818-2823.
7) Chen Y, Chen S, Liu LY, Zou ZL, Cai YJ, Wang JG, Chen B, Xu LM, Lin Z, Wang XD, Chen YP. Mesenchymal stem cells ameliorate experimental autoimmune hepatitis by activation of the programmed death 1 pathway. Immunol Lett 2014; 162(2 Pt B): 222-228.
8) Sakaguchi K, Kitano M, Nishimura M, Senoh T, Ohta T, Terao M, Shinji N, Koide N, Tsuji T. Serum level of transforming growth factor-beta1 (TGF-beta1) and the expression of TGF-beta receptor type II in peripheral blood mononuclear cells in patients with autoimmune hepatitis. Hepatogastroenterology 2004; 51: 1780-1783.
9) Leask A, Abraham D. TGF-beta signaling and the fibrotic response. FASEB J 2004; 18: 816-827.
10) Xu F, Liu C, Zhou D, Zhang L. TGF-β/SMAD Pathway and Its Regulation in Hepatic Fibrosis. J Histochem Cytochem 2016; 64: 157-167.
11) Kim SJ, Angel P, Lafyatis R, Hattori K, Kim KY, Sporn MB, Karin M, Roberts AB. Autoinduction of transforming growth factor beta 1 is mediated by the AP-1 complex. Mol Cell Biol 1990; 10: 1492-1497.
12) Ooshio T, Irie K, Morimoto K, Fukuhara A, Imai T, Takai Y. Involvement of LMO7 in the association of two cell-cell adhesion molecules, nectin and E-cadherin, through afadin and alpha-actinin in epithelial cells. J Biol Chem 2004; 279: 31365-31373.
13) Cenciarelli C, Chiaur DS, Guardavaccaro D, Parks W, Vidal M, Pagano M. Identification of a family of human F-box proteins. Curr Biol 1999; 9: 1177-1179.
14) Hu Q, Guo C, Li Y, Aronow B, Zhang J. LMO7 mediates cell-specific activation of the Rho-myocardin-related transcription factor-serum response factor pathway and plays an important role in breast cancer cell migration. Mol Cell Biol 2011; 31: 3223-3240.
15) Holaska J, Rais-Bahrami S, Wilson K. Lmo7 is an emerin-binding protein that regulates the transcription of emerin and many other muscle-relevant genes. Human Mol Gen 2006; 15: 3459-3472.
16) Doycheva I, Watt KD, Gulamhusein AF. Autoimmune hepatitis: current and future therapeutic options. Liver Int 2019; 39: 1002-1013.
17) Lohse AW, Chazouilleres O, Dalekos G, Drenth J, Heneghan M, Hofer H, Lammert F, Lenzi M. EASL clinical practice guidelines: autoimmune hepatitis. J Hepatol 2015; 63: 971-1004.
18) Harrison L, Gleeson D. Stopping immunosuppressive treatment in autoimmune hepatitis (AIH): Is it justified (and in whom and when)? Liver Int 2019; 9: 610-620.
19) Gleeson D, Heneghan MA. British Society of Gastroenterology (BSG) guidelines for management of autoimmune hepatitis. Gut 2011; 60: 1611-1629.
20) Meier RP, Mahou R, Morel P, Meyer J, Montanari E, Muller YD, Christofilopoulos P, Wandrey C, Gonelle-Gispert C, Bühler LH. Microencapsulated human mesenchymal stem cells decrease liver fibrosis in mice. J Hepatol 2015; 62: 634-641.
21) Meier RP, Müller YD, Morel P, Gonelle-Gispert C, Bühler LH. Transplantation of mesenchymal stem cells for the treatment of liver diseases, is there enough evidence? Stem Cell Res 2013; 11: 1348-1364.
22) Tu H, Chen D, Cai C, Du Q, Lin H, Pan T, Sheng L, Xu Y, Teng T, Tu J, Lin Z, Wang X, Wang R, Xu L, Chen Y. microRNA-143-3p attenuated development of hepatic fibrosis in autoimmune hepatitis through regulation of TAK1 phosphorylation. J Cell Mol Med 2020; 24: 1256-1267.
23) Zhan Y, Kim S, Yasumoto H, Namba M, Miyazaki H, Iwao H. Effects of dominant-negative c-Jun on platelet-derived growth factor-induced vascular smooth muscle cell proliferation. Arterio Thromb Vasc Biol 2002; 22: 82-88.

24) Cao X, Ross FP, Zhang L, MacDonald PN, Chappel J, Teitelbaum SL. Cloning of the promoter for the avian integrin beta 3 subunit gene and its regulation by 1,25-dihydroxyvitamin D3. J Biol Chem 1993; 268: 27371-27380.

25) Xie Y, Ostriker AC, Jin Y, Hu H, Sizer AJ, Peng G, Morris AH, Ryu C, Herzog EL, Kyriakides T, Zhao H, Dardik A, Yu J, Hwa J, Martin KA. LMO7 is a negative feedback regulator of transforming growth factor β signaling and fibrosis. Circulation 2019; 139: 679-693.

26) Lu FB, Chen DZ, Chen L, Hu ED, Wu JL, Li H, Gong YW, Lin Z, Wang XD, Li J, Jin XY, Xu LM, Chen YP. Attenuation of experimental autoimmune hepatitis in mice with bone mesenchymal stem cell-derived exosomes carrying microRNA-223-3p. Mol Cells 2019; 42: 906-918.

27) Tan CY, Lai RC, Wong W, Dan YY, Lim SK, Ho HK. Mesenchymal stem cell-derived exosomes promote hepatic regeneration in drug-induced liver injury models. Stem Cell Res Ther 2014; 5: 76-89.

28) Trop-Steinberg S, Azar Y. AP-1 expression and its clinical relevance in immune disorders and cancer. Am J Med Sci 2017; 353: 474-483.

29) Le Blanc K, Mougiakakos D. Multipotent mesenchymal stromal cells and the innate immune system. Nature Rev Immunol 2012; 12: 383-396.

30) Kang S, Xu H, Duan X, Liu JJ, He Z, Yu F, Zhou S, Meng XQ, Cao M, Kennedy GC. PCD1, a novel gene containing PDZ and LIM domains, is overexpressed in several human cancers. Cancer Res 2000; 60: 5296-5302.

31) Nakamura H, Mukai M, Komatsu K, Tanaka-Okamoto M, Itoh Y, Ishizaki H, Tatsuta M, Inoue M, Miyoshi J. Transforming growth factor-beta1 induces LMO7 while enhancing the invasiveness of rat ascites hepatoma cells. Cancer Lett 2005;220(1):95-99.